High gain dual-polarised pentagonal microstrip antenna for wireless communications

Raghunath Subhanrao Bhadade* and
Shrinivas Padmakar Mahajan

Department of Electronics and Telecommunication Engineering,
College of Engineering Pune,
Wellesley Road, Shivajinagar, Pune,
Maharashtra 411005, India
Email: raghunath.bhadade@mitpune.edu.in
Email: spm.extc@coep.ac.in
*Corresponding author

Abstract: In this paper we propose a dual polarised pentagonal microstrip antenna for massive MIMO-base station to operate at 2.4 GHz WLAN band (IEEE 802.11 b/g/n/ax). The various researchers have used antenna array with different feeds for the massive MIMO BS to obtain the desired gain with required impedance bandwidth. However, this proposed work contradicts with existing method by using a single novel radiating element with suspended substrate to achieve the desired gain and required impedance bandwidth. The circular polarisation is achieved by using two coaxial-probe feeds. The main focus of research is on the selection of proper shape of the radiating element for Massive MIMO BS. The proposed antenna is successfully simulated using HFSS 13.0, fabricated on a FR-4 substrate and measured. The proposed antenna exhibits a much higher gain of 6.17 dB, improved impedance bandwidth of 171.9 MHz (return loss, S11= –10 dB), the axial ratio (AR) is 1.78 dB (< 3 dB), the patch area of 1,775 mm^2, and also yields return loss better than –15 dB around the centre frequency of 2.45 GHz. The measured characteristics of the antenna are in good agreement with the simulated results.

Keywords: microstrip antenna; gain; input impedance; return loss.

Reference to this paper should be made as follows: Bhadade, R.S. and Mahajan, S.P. (2019) 'High gain dual-polarised pentagonal microstrip antenna for wireless communications', *Int. J. Ultra Wideband Communications and Systems*, Vol. 4, No. 1, pp.22–31.

Biographical notes: Raghunath Subhanrao Bhadade received his BE in 2000 from the Dr. B.A.M.U., Aurangabad and MTech in 2008 from the University of Pune. He is working as an Assistant Professor in Department of Electronics and Communication Engineering of Dr. Vishwanath Karad MIT-World Peace University, Pune, Maharashtra, India. He has 18 years of teaching experience. He is currently pursuing his PhD in Massive MIMO Antenna from the College of Engineering, Pune. His area of interest is RF, microwave and antennas, software defined radio, analogue/digital communication.

Shrinivas Padmakar Mahajan did his BE in 1991 from Marathwada University Aurangabad and subsequently completed PG and PhD with College of Engineering Pune, University of Pune, in 1996 and 2011, respectively. He has around 26 years of teaching experience in the same college and presently working as Associate Professor in Electronics and Telecommunication. His area of interest and research are Microwaves, Antennas and Signal Processing.

1 Introduction

Microstrip antennas play a crucial role in wireless applications such as LTE, Wi-MAX, WLAN and Wi-Fi. The low gain and impedance bandwidth is the serious limitation of these antennas in their conventional form.

Higher and higher data rates are to be provided by the modern communication systems. Significant increase in data throughput and link reliability without boosting the transmiter power or extra bandwidth is achieved by MIMO that happens to be the need of wireless communications.

Massive MIMO serves tens of terminals in the same time-frequency resource using antenna arrays with few hundred radiating elements in the structure. Aggressive spatial multiplexing is used in massive MIMO for increasing the capacity. Thus, more antennas, more capacity, and enhanced reliability (Yuan et al., 2017; Harris et al., 2017). Energy can be focused into smaller regions of

space by using extra antennas which in turn bring enormous improvements in radiated energy efficiency and throughput by leveraging time-division multiplexing (TDD) used in massive MIMO. Massive MIMO is scalable to any desired degree on the number of service antennas (Ngo et al., 2013; Larsson et al., 2014; Boccardi et al., 2014). The compact and low profile, low mutual coupling, high gain to reduce cost of RF chains, centralised and distributed, Multi mode, and multi frequency bands are some of the major challenges for Massive MIMO BS antennas.

In this paper we present the design, simulation, fabrication and validation of the proposed pentagon microstrip antenna for 1 × 1 MIMO at 2.4 GHz WLAN band. The remainder of this paper is structured as follows: Section 2 details the various radiating elements; Section 3 addresses the proposed antenna geometry; Section 4 presents the validation of the model and discussions; this is followed by, conclusions in Section 5, and future work in Section 6 respectively.

The design and development of optimal geometry of radiating element (modified pentagon) with the gain more than 6 dB having impedance bandwidth more than 170 MHz at 2.45 GHz is a useful achievement. These contributions by the authors will make a significant impact in overall development of massive MIMO BS antenna used for future wireless communications.

2 Radiating elements

The selection of radiating element for the massive MIMO BS based on the challenges plays a vital role. In this section we present the simulation of circular, triangular, and various regular polygons (pentagon to decagon) microstrip antennas. The existing radiating elements (rectangular and square) with the proposed antenna for the Massive MIMO BS are compared in Table 7. The borsight gain, impedance bandwidth, and area (compactness) of these antennas were compared.

The radiating patch (or element) design starts from the selection of the centre frequency of the band of operation. For demonstration purpose 2.45 GHz is chosen in the present study. The coaxial probe feed is used to excite the antenna. The input impedance level can be adjusted through the positioning of the feed points. All geometries of radiating elements were simulated with the probe dimensions (inner conductor of 0.65 mm, dielectric of 0.85mm and the outer conductor of 1.5 mm) of a commercially available SMA connector. The FR-4 substrate (cheaper than other substrates) is used for all the simulations, analysis and fabrication of the antenna with dielectric constant of 4.4, loss tangent of 0.0027 and thickness of 1.6 mm. The antenna parameters are optimised at 2.45 GHz. The ground plane has the dimensions of 60 × 60 mm. All parameters of the various radiating elements are optimised using HFSS 13.0 which is a finite element method (FEM) solver for electromagnetic (EM) structures.

2.1 Circular microstrip antenna

The dimensions of this antenna can be calculated by using the equation (1)

$$r = 1.8412c \Big/ 2\pi fr\left(\sqrt{\varepsilon_r}\right) \tag{1}$$

where 'r' is the radius of the circular microstrip antenna, c is the velocity of EM waves in free space, fr and ε_r are the resonant frequency and relative dielectric constant of the substrate respectively.

2.2 Triangular microstrip antenna

The dimensions of the triangular microstrip antenna can be calculated from the equation (2)

$$s = 2c \Big/ nfr\left(\sqrt{\varepsilon_r}\right) \tag{2}$$

where 's' is the length of side of radiating patch. The value of n is 3 for triangular microstrip antenna. The area of this antenna can be estimated by using equation (3). The simulated gain and bandwidth for the circular and triangular microstrip antenna are compared in Table 1.

Table 1 Simulated results for circular and triangular microstrip antennas for 2.45 GHz

Name of antenna	*Theoretical values*		*Simulated values*		*Boresight gain at the centre frequency of the operating band (dB)*	*Bandwidth (MHz) (VSWR = 2) (%)*
	Dimensions (mm)	*Area of patch (mm^2)*	*Dimensions (mm)*	*Area of patch (mm^2)*		
Circular	r = 17.2	929.40	r = 17.2	929.40	2.10	50 (2.04)
Triangular	S = 38.91	655.57	S = 38.45	640.21	1.61	(1.64)

Table 2 Simulated results for various regular polygons for 2.45 GHz

Name of polygon	*Number of sides (n)*	*Theoretical values*		*Simulated values*		*Boresight gain at the centre frequency of the operating band (dB)*	*Bandwidth (MHz) (S_{11} = –10 dB) (%)*
		Length of side (mm)	*Area of patch (mm^2)*	*Length of side (mm)*	*Area of patch (mm^2)*		
Pentagon	5	23.35	938.06	22.51	871.93	2.62	50 (2.04)
Hexagon	6	19.45	982.85	18.40	879.60	2.13	50.5 (2.06)
Heptagon	7	16.67	1,009.82	15.70	896.47	2.07	50 (2.04)
Octagon	8	14.97	1,027.81	13.47	876.82	2.09	53.3 (2.17)
Nonagon	9	12.97	1,039.91	11.94	882.35	2.26	53.3 (2.17)
Decagon	10	11.67	1,047.86	10.83	884.92	2.26	53.3 (2.17)

2.3 Regular polygon microstrip antenna

The regular polygon (five sided pentagon) microstrip antenna with single coaxial probe feed is shown in Figure 1. The length of side of the various regular polygons can be calculated from the equation (2). Area of the various regular polygons can be calculated from either the length of side or a radius (circumradius) or an apothem (inradius). Area of the radiating patch from the given length of side is given by the equation (3)

$$\text{Area} = \left(s^2 n\right) / \{4\tan(180^\circ / n)\} \tag{3}$$

The results intended for various regular polygons (n = 5 to 10) in terms of boresight gain, impedance bandwidth, and area of patch is given in Table 2.

Figure 1 Basic geometry of regular polygon (see online version for colours)

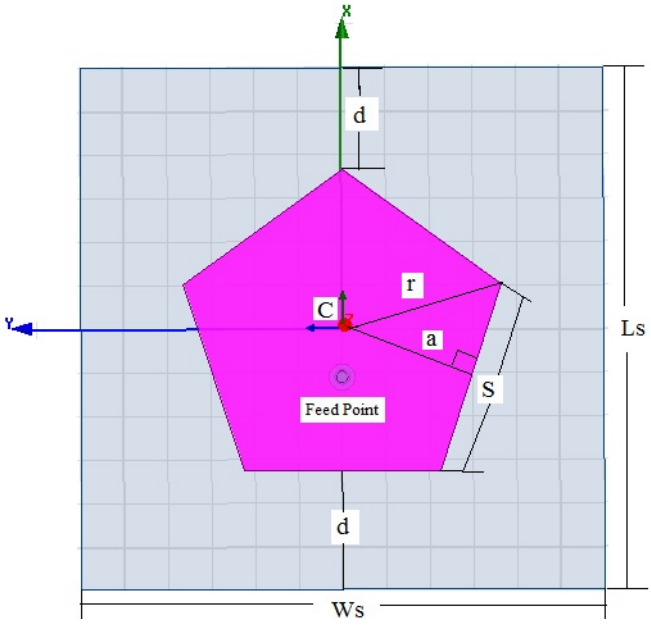

Notes: Centre of the polygon (C): feed point position = (–5.55, 0) mm; radius (r) = 18.33 mm; apothem (a) = 14.26 mm; length of side (s) = 22.51 mm; length of substrate (Ls) = 60 mm; width of substrate (Ws) = 60 mm; distance (d) = 11.67 mm.

It is apparent from Tables 2 and 3 that, the pentagonal microstrip antenna shows improved results in terms of the boresight gain of 2.62 dB, impedance bandwidth of 50 MHz (2.04%) at 2.45 GHz with smaller patch area of 871.93 mm^2 as compared to other radiating elements (Table 1). The simulated bandwidth provided by the pentagonal microstrip antenna would support to carry the required data rates at 2.4 GHz WLAN band for IEEE 802.11 b/g/n standards but not for IEEE 802.11 ax standard.

Table 3 Simulated results for pentagon microstrip antenna with air-gap for 2.45 GHz

Theoretical values		*Simulated values*		*Boresight gain at the centre frequency of the operating band (dB)*	*Bandwidth (MHz) (S_{11}= –10 dB) (%)*
Length of side (mm)	*Area of patch (mm^2)*	*Length of side (mm)*	*Area of patch (mm^2)*		
44.82	3,456	33.50	1,931	6.58	168 (7.06)

3 Proposed antenna

Linear polarisation (LP) is normally provided by the microstrip antennas; however, the circular polarisation (CP) can also be obtained by certain modifications to the basic antenna geometry and/or feed (Balanis, 2005). Dual polarised antennas are used to mitigate the multi-path effects and to improve communications capacity and quality (Garg et al., 2001). The dual polarised antennas in massive MIMO BS can serve many tens of terminals in the same time-frequency resource. CP radiation from the pentagonal microstrip antenna is obtained by using dual feed points (feed point 1 and 2). The two feeds encompass identical amplitude but in-phase quadrature. The quality of the CP antennas is specified by the axial ratio (AR). The proposed antenna supports dual polarisation (LP and RHCP) is shown in Figure 2. The LHCP can be obtained by shifting the position of feed pint 2 to (0, 5.8) mm.

Figure 2 Dual polarised pentagonal microstrip antenna (see online version for colours)

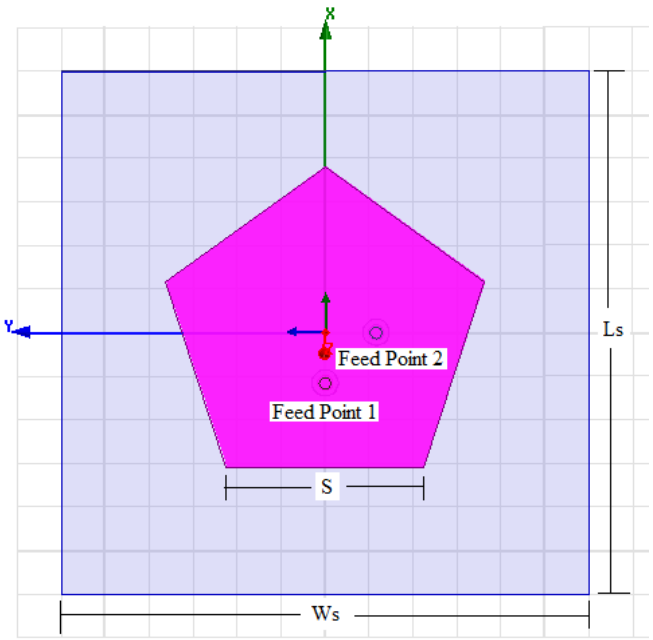

Notes: Feed point 1 position = (–5.8, 0) mm; feed point 2 position = (0, 5.8) mm; length of side (s) = 22.45 mm; radius (r) = 19.1 mm; apothem (a) = 15.4 mm; area of patch = 867.3873 mm^2; Ws = 60 mm; Ls = 60 mm; d = 10.9 mm.

The radiation pattern (E-plane and H-plane) and the S-parameters (S11, S12 or S21, and S22) of this antenna are given in Figure 3 and 4 respectively. The antenna has more gain along the z-direction (intended) and has very small back lobe opposite to the main beam direction. The simulated return loss (S11 and S12) are better than –22 dB and isolation (S12) is more than 40 dB.

The co-polarisation and cross-polarisation of this antenna is shown in Figure 5. The co-polarised far-field component has the similar polarisation as the excitation. The cross-polarised far-field component is orthogonal to co-polarised component and main lobe direction. If the cross polarisation is vertical, the antenna is horizontally polarised. Similarly, If the cross polarisation is left hand circularly polarised (LHCP), the antenna polarisation is right hand circularly polarised (RHCP). To indicate how many decibels below the desired polarisation's power level the cross polarisation power level is, one may specified cross polarisation power level in negative dB.

Figure 3 Simulated radiation pattern of dual polarised pentagonal microstrip antenna (see online version for colours)

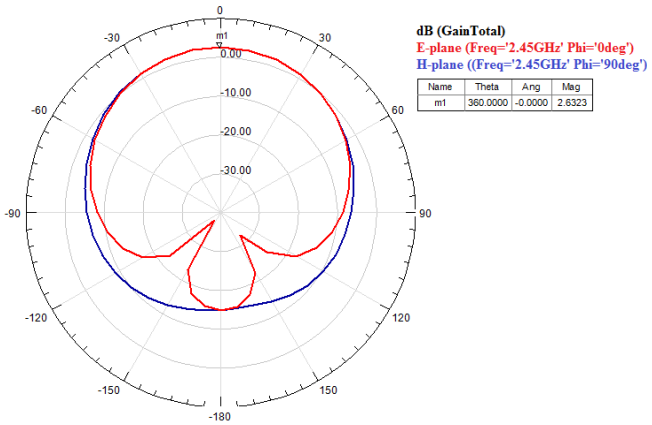

Note: Gain = 2.6323 dB and HPBW = 80°.

Figure 4 Simulated S – parameters for dual polarised pentagonal microstrip antenna (see online version for colours)

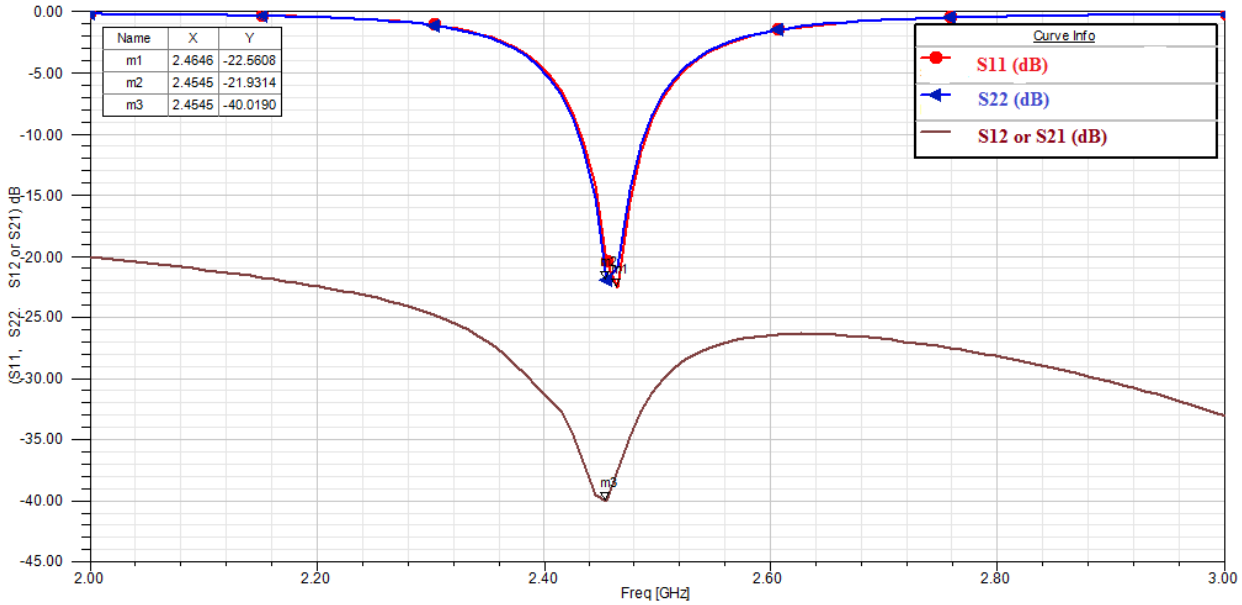

Notes: S_{11} = -22.5608 dB; S_{12} = S_{21} = –40.0190 dB; S_{22} = –21.9314 dB; bandwidth (S_{11} = -10dB) = 50MHz.

Figure 5 Simulated co-polarisation and cross-polarisation radiation pattern (see online version for colours)

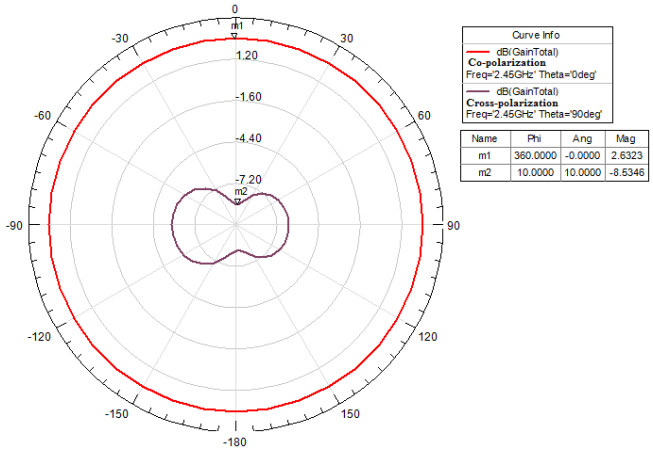

Figure 6 Proposed dual polarised pentagonal microstrip antenna, (a) top view (b) cross sectional view (see online version for colours)

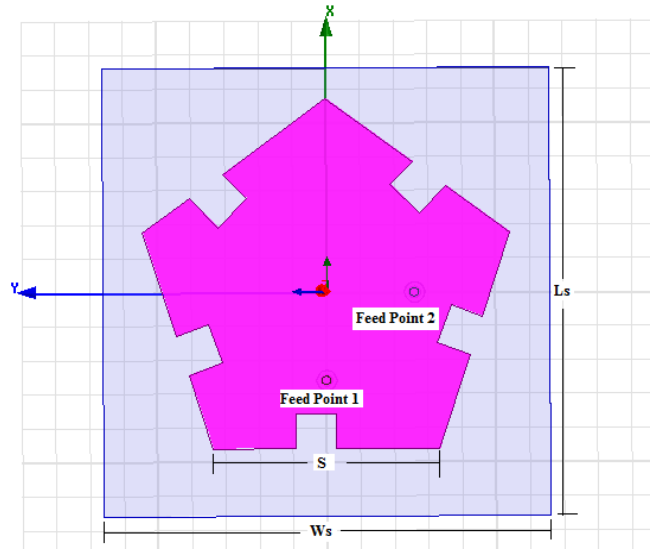

(a)

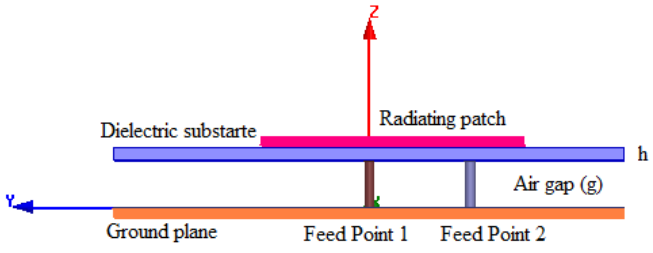

(b)

Notes: Feed point 1 position = (–13, 0) mm; feed point 2 position = (0, –13) mm; length of side (s) = 33.50 mm; radius (r) = 28.5 mm; apothem (a) = 23.05 mm; Ws = 66 mm; Ls = 66 mm.

The basic geometry of the proposed pentagonal microstrip for 1 × 1 MIMO antenna is shown in Figure 6. The sufficient gain and required impedance bandwidth at 2.4 GHz WLAN band (IEEE 802.11 ax) is achieved by using the suspended substrate technique.

This antenna employs an air gap layer of thickness 'g' between the dielectric substrate and ground plane. The presence of an air gap reduces the effective dielectric constant for the antenna, giving rise to an increase in resonant frequency and impedance bandwidth. The adjustable air-gap thickness can be used to reduce the effective loss of a lossy substrate and to tune the antenna frequency (Garg et al., 2001). Also, decrease in ε_r of the substrate can be used to increase the gain of the antenna (Pang et al., 2014; Vieira et al., 2014). A long pin SMA connector is used to excite the radiating patch. The length of side 's' of the patch can be calculated by the using equation (3) with substitution of ε_r by ε_{re} which is called effective relative permittivity of the two-layered cavity (Garg et al., 2001) given by equation (4)

$$\varepsilon_{re} = \varepsilon_r (h+g)/(h+\varepsilon_r g) \tag{4}$$

Use of air-gap enhances the impedance bandwidth exclusive of escalating the size and complexity of the radiating patch too much. In Kasabegoudar and Vinay (2010, 2004), the antenna's impedance bandwidth was maximised by using the expression (5)

$$g = 0.16\lambda_0 - h\sqrt{\varepsilon_r} \tag{5}$$

where 'g' is the air gap above the ground plane, λ_0 is wavelength in free space. The optimum value of the air-gap is 6 mm (Kasabegoudar and Vinay, 2004). The dual polarised pentagon microtsrip antenna is simulated using the air-gap of 6 mm. The results for this antenna are given in Table 3.

Table 4 Optimisation of five slits for 2.45 GHz

Five slits dimensions (mm)		*Boresight gain at the centre frequency of the operating band (dB)*	*Bandwidth (MHz) (S_{11} = –10 dB) (%)*
Length (L)	*Width (W)*		
1	1	6.55	143 (5.83)
2	2	6.57	143 (5.83)
3	3	6.57	140 (5.71)
4	4	6.21	168 (6.85)
5	5	6.16	173 (7.07)

Table 5 Final dimensions of the proposed antenna design for 2.45 GHz

Parameter	*Value*
Length of side of radiating patch (s)	33.50 mm
Length of five slits (L)	5.0 mm
Width of five slits (W)	4.0 mm
Air gap between substrates (g)	6.0 mm
Relative dielectric constant (ε_r)	4.4
Thickness of substrate (h)	1.6 mm
Loss tangent	0.0027
Ground plane (Ls × Ws)	66 × 66 mm

From Table 4 it is clear that, with the air-gap of 6 mm, the proposed pentagon microstrip antenna shows enhanced gain of 6.58 dB and improved impedance bandwidth of 168 MHz (7.06%) as compared to pentagon microstrip antenna without air-gap (Table 2).

The area of the proposed antenna is reduced by loading of the slits on the radiating patch (Garg et al., 2001). The dual polarised suspended pentagonal microstrip antenna loaded with five slits is shown in Figure 7. The five slits created based on the current distribution on the radiating patch.

Figure 7 Proposed dual polarised pentagonal microstrip antenna (see online version for colours)

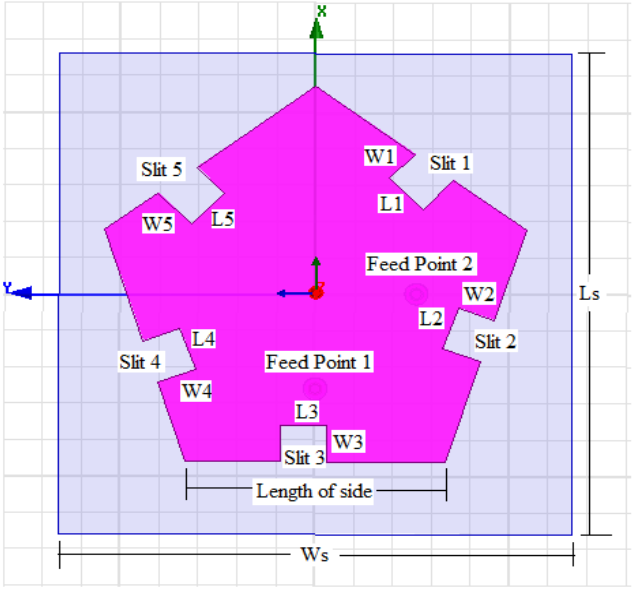

Notes: Feed point 1 position = (–13, 0) mm; feed point 2 position = (0, –13) mm; length of side (s) = 33.50 mm; radius (r) = 29.49 mm; apothem (a) = 23.05 mm; Ws = 66 mm; Ls = 66 mm.

The slits dimensions (L and W) were varied to achieve the optimum value of gain and impedance bandwidth. In the first step, slits length and width was kept to 1 mm (Table 5) and later the slits dimensions were varied in a step of 1mm. The variation in simulated gain and impedance bandwidth for each one is specified in Table 4. Based on these studies it can be noted that the optimum slits length and width are 5mm and 4mm respectively.

Figure 8 Simulated radiation pattern of dual polarised pentagonal microstrip antenna (see online version for colours)

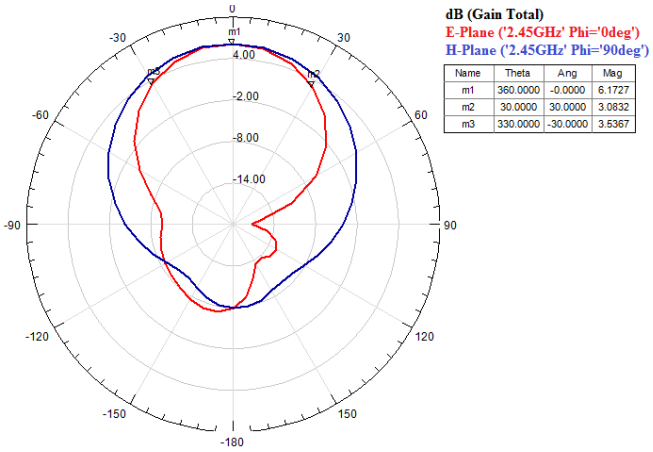

Note: Gain = 6.17 dB, HPBW = 60°.

The simulated E-plane (absolute) and H-plane (absolute) field patterns of the proposed antenna is given in Figure 8 for x-y plane. For the optimum slit dimensions, the simulated gain of 6.17 dB, impedance bandwidth of 171.9 MHz with reduction in patch area of 1,775 mm^2 is obtained as compared to the microstrip antenna without five slits (Table 3).

Figure 9 Simulated axial ratio vs frequency plot (see online version for colours)

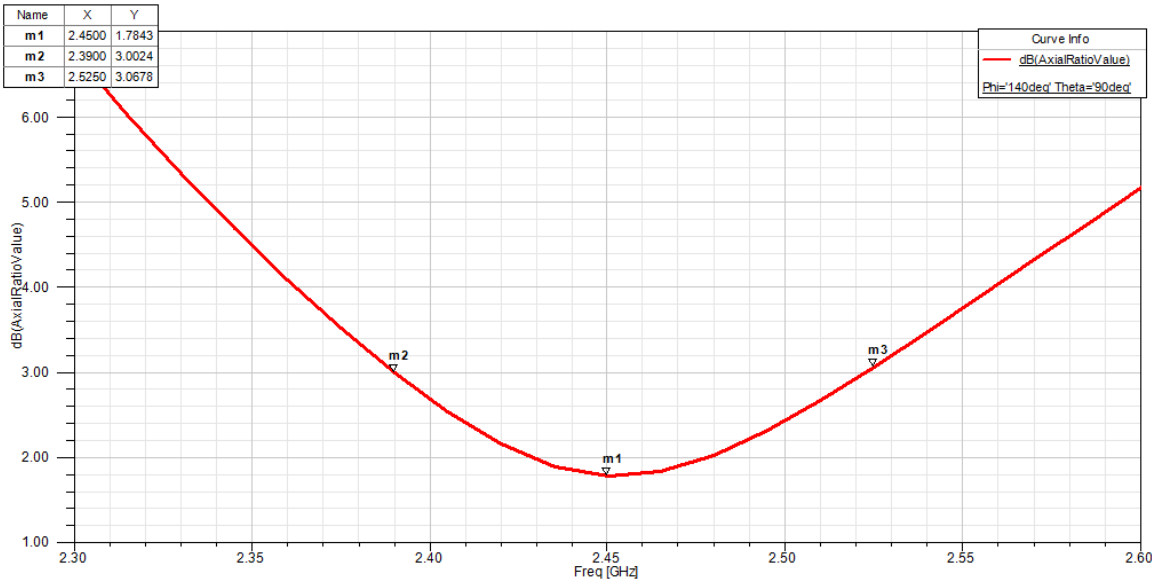

Table 6 Comparison of various characteristics of simulated and measured prototype

Parameters	*Feed point 1*		*Feed point 2*	
	Simulated	*Measured*	*Simulated*	*Measured*
Resonant frequency (GHz)	2.45	2.53	2.45	2.53
Gain (dB)	6.17	6.01	6.17	6.01
S_{11} (dB)	–16.12	–15.34		
S_{12} or S_{21} (dB)	–19.60	–21.35	–19.60	–21.35
S_{22} (dB)			–16.11	–21.35
Impedance bandwidth (S_{11} = –10 dB) (MHz) (%)	171.9 (7.01%)	169.2 (6.68%)	181.3 (7.40%)	179.9 (7.11%)
VSWR	1.370	1.414	1.371	1.076
Phase (degrees)	90.71	87.92	90.71	87.92
Input impedance (ohms)	63.5	66.44	63.5	52.96

Figure 10 Fabricated prototype geometry, (a) top view (b) bottom view (c) side view (see online version for colours)

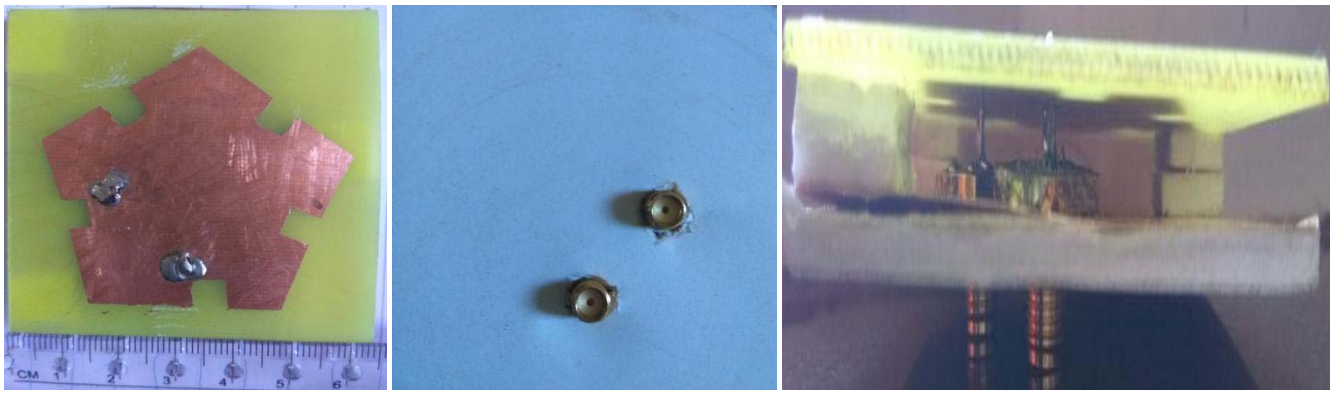

(a) (b) (c)

The AR plot of the proposed antenna is shown Figure 9. The value of AR is 1.78 dB (< 3dB) and AR bandwidth 135 MHZ is achieved. The AR bandwidth is narrower than the impedance bandwidth, as this is usual for microstrip antennas. The final dimensions of the proposed pentagonal microstrip antenna are given in Table 5.

4 Validation of the model and discussions

The dual polarised prototype was fabricated as designed in the previous section with dimensions described in Table 6 and one such prototype is shown in Figure 10. A foam material (white in colour) is placed below the ground plane to maintain the flatness of the ground so as to have uniform current distribution over the ground. As a result, the foam influences the effective dielectric constant and hence the resonant frequency slightly deviated.

The experimental set up for the measurement of radiation pattern and gain of the prototype pentagon antenna is as shown in Figure 11. The calibrated vector network analyser (Agilent, 8714ET) is used as an excitation source for the standard dipole antenna (transmitting). The power of the excitation source was set to 0 dBm at 2.45 GHz. The Spectrum analyser (Keysight, N9320B) is used as a receiver for the measurement of received signal strength at 2.45 GHz.

Figure 11 Experimental set up, (a) outdoor (b) indoor (see online version for colours)

(a)

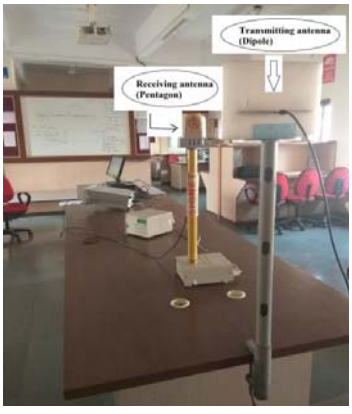

(b)

The fabricated pentagonal microstrip antenna (Receiving) was rotated from 0° to 360° in a step of 10° with the help of stepper motor. The height of both the antenna was set to 15λo (λo is 12 cm at 2.45 GHz). The received signal strength was measured using a spectrum analyser. The normalised received strength (dBμV) is plotted as a function of theta (degree). The measured radiation pattern for co-polarisation (horizontal) of the receiving antenna at far-field plotted in a linear form is as shown in Figure 12.

The radiation pattern for co-polarisation (horizontal) and cross-polarisation (vertical) of this antenna at the far-field shows the good agreement with indoor measurement. Also, the antenna exhibits 80° half-power beam-width at far-field. The boresight gain of fabricated antenna was measured by using two-antenna method. For the indoor experimental set up, the frequency of excitation source and spectrum analyser was varied from 2 GHz to 3 GHz in a step of 100 MHz. Initially measurements were done using a standard dipole antenna and then with the fabricated pentagonal microstrip antenna. The boresight gain of this antenna was calculated from the received signal strength and then it is compared to the gain of dipole antenna. The measured boresight gain of this antenna is 6.01 dBd (with respect to dipole) at 2.45 GHz is as shown in Figure 13.

A calibrated two-port vector network analyser (Agilent, N9923A) is used to measure all the S-parameters, Impedance bandwidth, VSWR, Phase, and Input impedance. The measured return loss of the fabricated antenna is given in Figure 14. The measured return loss is below −15 dB in the operating range (2.44–2.61 GHz). The measured impedance bandwidth of 170 MHz would support the required data rates at 2.4 WLAN band (IEEE 802.11 b/g/n/ax).

Figure 12 Simulated and measured radiation pattern of prototype for the frequency of 2.45GHz (see online version for colours)

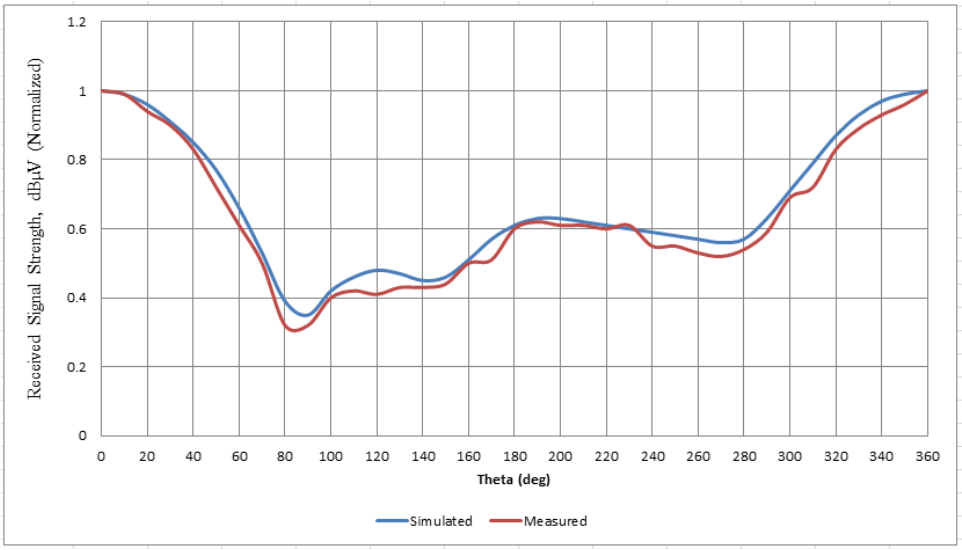

Figure 13 Simulated and measured gain vs. frequency (see online version for colours)

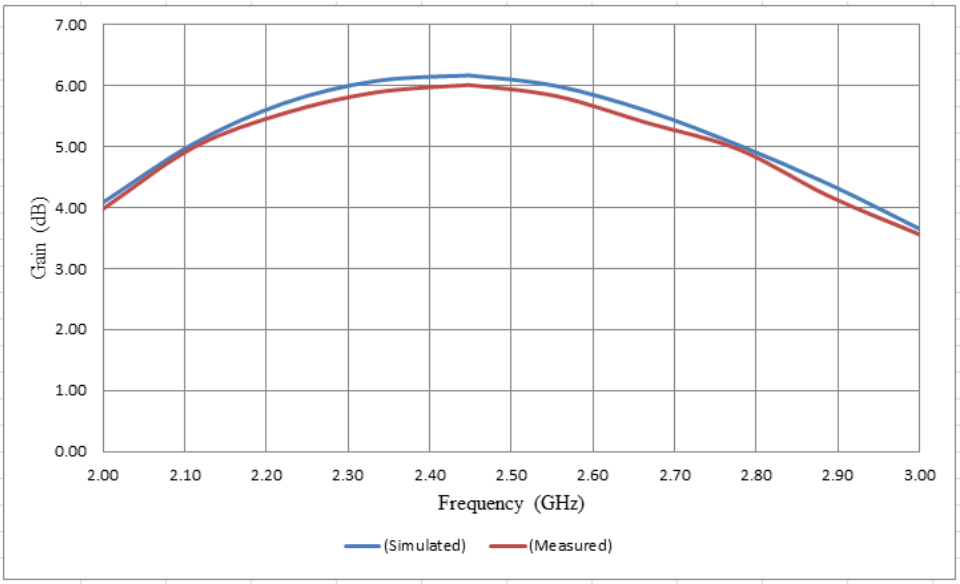

Figure 14 Simulated and measured return loss (S_{11}) of prototype (see online version for colours)

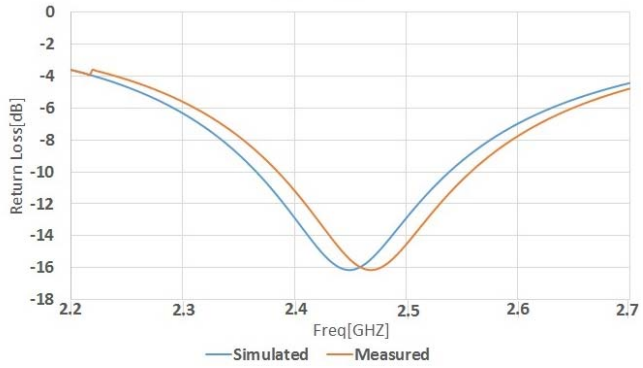

Figure 15 Measured input impedance vs frequency (feed point 1) (see online version for colours)

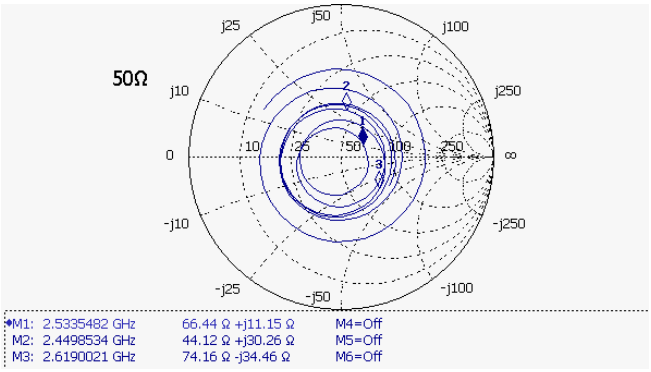

Figure 16 Measured VSWR Vs frequency (feed point 1) (see online version for colours)

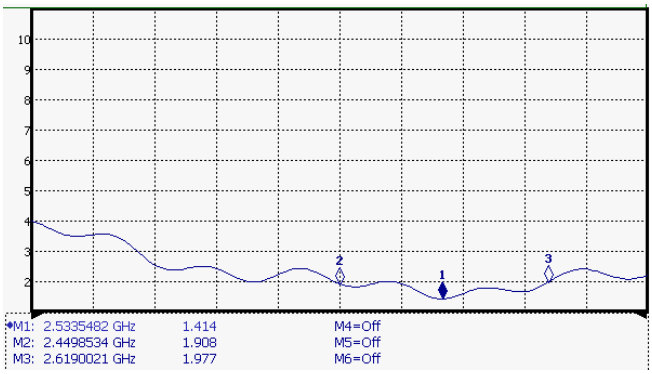

Figure 17 Measured phase vs frequency (between feed point 1 and 2) (see online version for colours)

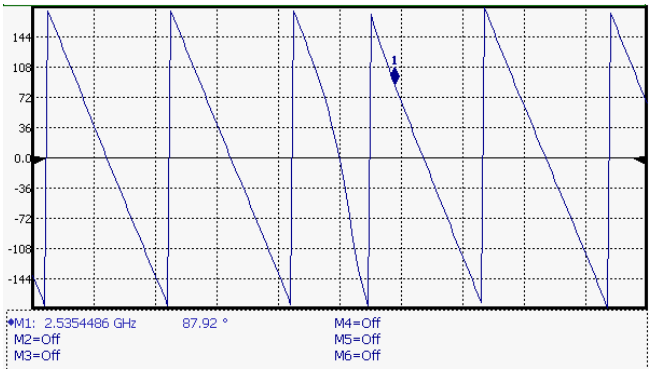

Figure 18 Measured mutual coupling (S_{12} or S_{21}) Vs frequency (between Feed point 1 and 2) (see online version for colours)

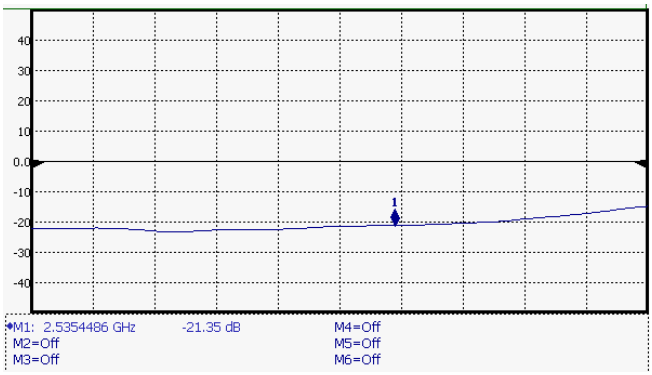

The measured input impedance, VSWR, phase, and mutual coupling of the fabricated antenna are illustrated in Figure 15, 16, 17, and 18 respectively. The comparisons of all the results (simulated and measured) are listed in Table 6. It can be observed that, the measured results agree with the simulated ones.

Table 7 Benchmarking results of the antennas with literature

Referenced antennas	*Operating frequency (GHz)*	*Gain (dB)*	*Bandwidth (MHz)*
Al-Tarifi et al. (2016)	3.6	5.4 / port (2 × 2 antenna array)	230
Pang et al. (2014)	5.8	13 / port (1 × 4 antenna array)	200
Kim et al. (2014)	2.596	10 / port (1 × 4 antenna array)	194
Vieira et al. (2014)	3.7	Not mentioned	185
Payami and Tufvesson (2012)	2.6	Not mentioned	50
Proposed antenna	2.45	6.17 / port (without antenna array)	171.9

Table 7 demonstrates a comparison of various radiating elements used for the Massive MIMO BS. In Al-Tarifi et al. (2016), the rectangular microstrip antenna (2 × 2 antenna array with edge-feed and LP) was used to obtain the gain of 5.4 dB per port (total four antennas) and impedance bandwidth of 230 MHz. The rectangular microstrip antenna (1 × 4 antenna array with in-set feed and LP) was proposed to obtain the gain of 13 dB per port (total four antennas) and impedance bandwidth of 200 MHz (Pang et al., 2014). In Kim et al. (2014), the square microstrip antenna (1 × 4 antenna array with corporate-feed and LP) was investigated to achieve the gain of 10 dB per port (total four antennas) and impedance bandwidth of 194 MHz. It is seen from our design, by using a coaxial-feed, dual polarisation (LP and RHCP), suspended substrate, slits loading on the patch and without using an antenna array; the single pentagonal microstrip antenna exhibits a gain of 6.17 dB per port and impedance bandwidth of 171.9 MHz.

5 Conclusions

The developed pentagonal microstrip antenna is proposed for massive MIMO BS to operate at 2.4 GHz WLAN band (IEEE 802.11 b/g/n/ax). The suspended substrate has been shown previously to improve the antenna's gain and impedance bandwidth. The five slits were optimised to maximise the gain and impedance bandwidth with reduced area of the antenna. The proposed antenna geometry exhibits the return loss better than −15 dB, a gain of 6.17 dB, and impedance bandwidth of 171.9 MHz, AR of 1.78 (< 3 dB) at 2.45 GHz. The characteristics obtained with the HFSS simulation and experimental results are found to be in good agreement.

6 Future work

The massive MIMO BS antenna will be based on mounting the total number of 64 elements (or 128 ports) or 96 elements (or 192 ports) with no spatial correlation between pentagonal radiating elements on each side of the octagonal shaped architecture. The octagonal shaped architecture for BS antenna uses space more efficiently and has approximately 20% more space than a square with same perimeter. Each side of the octagon consists of either 8 or 12 elements. These 'uncoupled' radiating elements will be capable of producing mutually exclusive spatial-beams for the Massive MIMO BS antenna.

Acknowledgements

This work is supported by Center of Excellence in Signal and Image Processing of College of Engineering, Shivajinagar, Pune, Maharashtra, India.

References

Al-Tarifi, M.A., Faouri, Y.S. and Sharawi, M.S. (2016) 'A printed 16 ports massive MIMO antenna system with directive port beams', *IEEE 5th Asia-Pacific Conference on Antennas and Propagation (APCAP)*, pp.125–126.

Balanis, C.A. (2005) *Antenna Theory*, Chapter 2 and Chapter 14, John Wiley and Sons, Inc. Publications, Hoboken New Jersey.

Boccardi, F., Heath, R.W., Lozano, A., Marzetta, T.L. and Popovski, P. (2014) 'Five disruptive technology directions for 5G', *IEEE Communications Magazine*, Vol. 52, No. 2, pp.74–80.

Garg, R., Bhartia, P., Bahl, I. and Ittipiboon, A. (2001) *Microstrip Antenna Design Handbook*, Chapters 6, 8 and 9, Artech House Inc., 685 Canton Street Norwood, 02062, Massachusetts.

Harris, P., Joao Vieira, E., Bengtsson, F.T., Hasan, W.B., Liu, L., Beach, M. (2017) 'Performance characterization of a real-time massive MIMO system with LOS mobile channels', *IEEE Journal on selected areas in Communications*, Vol. 35, No. 6, pp.1244–1253.

Hoydis, J., Brink, S.T. and Debbah, M. (2013) 'Massive MIMO in the UL/DL of cellular networks: how many antennas do we need?', *IEEE Journal on Selected Areas in Communications*, Vol. 31, pp.160–171.

Kasabegoudar, V.G. and Vinay, K.J. (2004) 'A broadband suspended microstrip antenna for circulation polarization', *Progress in Electromagnetics Research*, Vol. 90, pp.353–368.

Kasabegoudar, V.G. and Vinay, K.J. (2010) 'Coplanar capacitively coupled probe fed microstrip antennas for wideband applications', *IEEE Transactions on Antennas and Propagation*, Vol. 58, No. 10, pp.3131–3138.

Kim, Y., Ji, H., Lee, J., Nam, Y-H., Ng, B.L., Tzanids, I., Yang, L. and Zhang, J. (2014) 'Full dimension MIMO (FD-MIMO): the next evolution of MIMO in LTE systems', *IEEE Wireless Communications*, Vol. 21, No. 3, pp.91–100.

Larsson, E.G., Edfors, O., Tufvesson, F. and Marzetta, T.L. (2014) 'Massive MIMO for next generation wireless systems', *IEEE Communications Magazine*, Vol. 52, No. 2, pp.186–195.

Ngo, H.Q., Larsson, E. and Marzetta, T. (2013) 'Energy and spectral efficiency of very large multiuser MIMO systems', *IEEE Transactions on Communications*, Vol. 61, No. 4, pp.1436–1449.

Pang, X., Hong, W., Yang, T. and Li, L. (2014) 'Design and Implementation of an active multibeam antenna system with 64 RF Channels and 256 antenna elements for massive MIMO application in 5G wireless communications', *China Communications*, Vol. 11, pp.16–23.

Payami, S. and Tufvesson, F. (2012) 'Channel measurements and analysis for very large array systems at 2.6 GHz', *European Conference on Antennas and Propagation (EUCAP' 2012)*, Prague, pp.433–437.

Vieira, J., Malkowsky, S., Nieman, K., Miers, Z., Kundargi, N., Liu, L. and Tufvesson, F. (2014) 'A flexible 100-antenna testbed for Massive MIMO', *IEEE Globecom Workshop*, Austin, Texas, USA.

Yuan, H-W., Cui, G-F. and Fan, J. (2017) 'A method for analyzing broadcast beamforming of massive MIMO antenna array', *Progress in Electromagnetics Research Letters*, Vol. 65, pp.15–21.